MICROMAGNETICS OF THIN FERROMAGNETIC FILMS UNDER MECHANICAL STRESS

P.A. VOLTAIRAS, D.I. FOTIADIS, C.V. MASSALAS

2-98

Preprint no. 2-98/1998

Department of Computer Science
University of Ioannina
451 10 Ioannina, Greece

Micromagnetics of Thin Ferromagnetic Films under Mechanical Stress

P. A. Voltairas†, D. I. Fotiadis†, C. V. Massalas‡
† Dept. of Computer Science, University of Ioannina, GR 451 10 Ioannina, Greece
‡ Dept. of Mathematics, University of Ioannina, GR 451 10 Ioannina, Greece
e-mail: {pvolter, fotiadis@cs.uoi.gr, cmasalas@cc.uoi.gr}

Abstract

Understanding micromagnetic processes in magnetic materials play a crucial role for the design of new magnetic storage devices with improved characteristics. Among the phenomena that are present in ferromagnetic materials, magnetostriction is the one that has not been studied in extent, due to its complexity. In this paper a simple model is presented to study the effect of magnetostriction on the magnetization reversal in ferromagnetic materials. The magnetization reversal mechanism is such that self-magnetostatic energy is minimized. To simplify the calculations the strains are assumed to be uniform and the ferromagnetic material is confined in a solid nonmagnetic matrix. The equilibrium equations of the magnetization are derived from the free energy density expression. The dependence of coherent reversal (Stoner-Wohlfarth Model-SWM), as well as of non-coherent reversal of the magnetization on the magnetoelastic constants is discussed. The effect of stress on the magnetization curve (well known as *inverse magnetostrictive effect*) is also studied selecting the proper boundary conditions. An analytical relation between coercivity and stress is obtained for coherent reversal model. From our analysis we conclude that the stress dependence of coercivity is at least qualitatively the same with related experiments.

Keywords: Micromagnetics; Magnetization Reversal; Nucleation Field; Thin Film, Mechanical Stress; Magnetostriction

1. INTRODUCTION

The magnetic behavior of ferromagnetic materials, based on micromagnetic theory, has been studied extensively during the last four decades for rigid specimens [1]. The coupled magnetoelastic phenomena are essential for the construction of efficient disc storage devices, actuator and sensor devices. The theoretical framework for the description of such coupled magnetomechanical phenomena was proposed by Brown [2] and an extensive literature is cited in Ref. [3]. The foundation of such an approach was due to the pioneering works of Tiersten [4-5], Brown [2, 6] and Maugin and Eringen [7-9]. Among the various phenomena that are present magnetostriction is the most promising for applications and still the most difficult to be described theoretically. In the classical literature this term denotes the deformation of a ferromagnetic crystal when it is cooled under the critical Curie temperature (*spontaneous magnetostriction*), or when on a previous saturated ferromagnetic crystal is applied an additional external field capable of increasing the spontaneous magnetization beyond its saturation value

(*forced magnetostriction*). Whether the ferromagnetic crystal is longer or shorter in the direction of the magnetization the material is characterized as having *positive* or *negative magnetostriction*, respectively. The inverse effect is present too. When a ferromagnetic specimen is under mechanical loading (tension or compression) a change is noticed in its magnetic structure (*inverse magnetostrictive effect*). The capability of an applied mechanical loading to produce net resulting magnetization in a previously demagnetized ferromagnetic specimen has been examined experimentally and theoretically by Misra [10]. A wide class of phenomena that relates the elastic properties of ferromagnetic materials with the magnetization are generally referred to as magnetostriction (Joule effect, Matteucci effect, Wiedemann effect, etc.) [11].

Recently, new mathematical tools have utilized (Young measure) in order to explain the large magnetostriction observed in a class of ferromagnetic materials [12-13]. Similar calculations were also performed by Simone [14]. The effect of magnetostriction on the magnetization reversal of an infinite cylinder was studied for the curling mode [15-16]. It was proven that magnetostriction does not affect the nucleation field of the infinite cylinder. Energy estimations confirmed that in that case the hysteresis curve is rectangular in shape. In a deformable ferromagnet the elastic constants depend on the magnetization, thus a nonlinear stress-strain law is followed [17]. Thermodynamic arguments have been applied to explain this nonlinearity, well known as ΔE effect [18-19].

The main purpose of the present work is to describe through a simple model the principal physical mechanism of direct and inverse magnetostrictive effect. More specifically we confine ourselves on the effect of stress on the magnetization reversal of thin film ferromagnetic specimens, since for this case there are recent available experimental results [20-25]. In order to simplify the calculations we adopt a one dimensional magnetization reversal mode that has the advantage of minimizing the self-magnetostatic energy. We assume uniform strains and that the external mechanical stress is applied perpendicular to the external field direction. These simple assumptions are capable of revealing the underlying physical mechanism for the effect of stress on the magnetization reversal (coercive force). Even in the coherent reversal (SWM) the effect of stress on the magnetization reversal is evident. Analytical coercivity-stress and remanence-stress laws were obtained for the coherent reversal model. Depending on the sign of the magnetoelastic constants, the theory is applicable to material that exhibit either positive or negative magnetostriction. The simplifying assumptions do not allow us to describe the size dependence on coercivity. Simple linearized calculations around the initial saturation state derive a linear dependence of the theoretically predicted nucleation field on stress, being tensile or compressive. Whether these departure modes, from the initial saturation state, will emerge under increased opposite applied field depends on the solution of the nonlinear problem, which for our model reduces to the computation of an elliptic integral.

2. THEORY OF MAGNETOELASTIC INTERACTIONS

The present analysis is based on the micromagnetic approach proposed by Brown [2]. This phenomenological theory uses information from the microstructure (quantum mechanical exchange interactions) and describes the behavior of the material through macroscopic quantities (exchange forces). In the micromagnetic theory the behavior of ferromagnetic materials is described through the magnetization vector $\boldsymbol{M}$ (magnetic dipole moment per unit volume) which is considered as a continuously distributed vector

$$M_i = M_S\, a_i, \quad a_i = a_i\left(x_j, t\right), \quad i,j = 1,2,3 \tag{1}$$

having a constant absolute value at every point

$$M_i M_i = M_S^2(T), \quad \left(a_i\, a_i = 1\right), \tag{2}$$

where M_S, and a_i denote the saturation magnetization per unit volume and the direction cosines of the magnetization vector, respectively. We note that (2) is valid for temperatures much lower than the Curie temperature $\left(T << T_C\right)$ where the ferromagnetic material switches to the paramagnetic phase. For deformable ferromagnets, M_i must be replaced by the magnetization vector per unit mass M_i, that is:

$$\mathsf{M}_i = M_i / \rho, \tag{3}$$

where ρ is the mass density. The ferromagnetic Gibbs free energy, at a given temperature, applied field $\boldsymbol{H}^\circ$, body force $\rho \boldsymbol{f}$, and surface force density $\boldsymbol{T}$, has the general expression, with respect to internal variables:

$$G = F + W_\mu + W_H + W_S - \iiint_V \rho\, f_i\, u_i\, dV - \iint_{\partial V} T_i\, u_i dS, \tag{4}$$

where:

$$W_\mu = -\frac{1}{2}\mu_\circ \iiint_V \rho_\circ\, H_i' \mathsf{M}_i\, dV_\circ, \qquad \text{(Magnetostatic-self energy)} \tag{5}$$

$$W_H = -\mu_\circ \iiint_V \rho H_i^\circ\, M_i\, dV, \qquad \text{(Zeeman energy)} \tag{6}$$

$$W_S = \frac{1}{2}\mu_\circ \iint_{\partial V} \rho^2\, K_S\, n_i n_j \mathsf{M}_i \mathsf{M}_j\, dS, \qquad \text{(Surface energy)} \tag{7}$$

$$F = \iiint_V \rho \mathsf{F}_{\text{loc}}\, dV, \qquad \text{(Helmholtz free energy)} \tag{8}$$

and $\boldsymbol{H}'$ is the field $\left(\boldsymbol{H}' = \boldsymbol{H} - \boldsymbol{H}^{\circ}\right)$ due to the presence of the magnetization $\boldsymbol{M}$, K_S is the surface magnetocrystalline anisotropy constant, $\boldsymbol{n}$ is the outward unit normal vector on ∂V and $\boldsymbol{u}$ is the displacement vector. We note that μ_o is the permeability of vacuum. Here and hereafter summation over repeated subscripts is understood.
The local part of the Helmholtz free energy $\mathrm{F}_{\mathrm{loc}}$, is assumed to have the functional form:

$$\mathrm{F}_{\mathrm{loc}} = \mathrm{F}_{\mathrm{loc}}\left(x_{i,A}, \mathrm{M}_i, \mathrm{M}_{i,A}\right), \tag{9}$$

where $x_{i,A}$ is the deformation gradient. $\mathrm{F}_{\mathrm{loc}}$ includes elastic, magnetocrystalline anisotropic, magnetoelastic and exchange energy terms.. The vanishing of the first variation of the free energy leads to mechanical and magnetic equilibrium equations, as follows:

Mechanical equilibrium equations

$$\begin{aligned} &t_{ij,j} + \mu_o M_j H_{i,j} + \rho f_i = 0, \quad \text{in } V \\ &t_{ij} n_j = \frac{1}{2}\mu_o M_n^2 n_i + T_i, \qquad \text{on } \partial V \end{aligned} \tag{10}$$

where t_{ij} is the stress tensor which is generally non-symmetric and $M_n \equiv n_i M_i$ represent the magnetic surface charges. The constitutive law for the material is [2,16]:

$$t_{ij} = \frac{\partial \mathrm{F}_{\mathrm{loc}}}{\partial e_{ij}} + \frac{\partial \mathrm{F}_{\mathrm{loc}}}{\partial a_i} a_j. \tag{11}$$

Magnetic Equilibrium equations

$$\begin{aligned} &\rho\, \mathbf{M} \times \boldsymbol{H}^{\mathrm{eff}} = 0, \quad \text{in } V \\ &\frac{\partial \mathbf{M}}{\partial n} = 0, \qquad \text{on } \partial V \end{aligned} \tag{12}$$

where $\partial/\partial n \equiv \boldsymbol{n} \cdot \nabla$ and $\boldsymbol{H}^{\mathrm{eff}}$ is the effective field that tends to keep the magnetization vector parallel to its direction and has components of the following form:

$$H_i^{\mathrm{eff}} = H_i - \frac{1}{\mu_o M_S}\left[\frac{\partial \mathrm{F}_{\mathrm{loc}}}{\partial a_i} - \frac{1}{\rho}\left(\rho \frac{\partial \mathrm{F}_{\mathrm{loc}}}{\partial a_{i,A}} x_{j,A}\right)_{,J}\right]. \tag{13}$$

The self-magnetostatic field $\boldsymbol{H}'(\equiv -\nabla\Phi)$ is the result of the volume $(\nabla\cdot\boldsymbol{M})$ and surface $(M_n \equiv \boldsymbol{n}\cdot\boldsymbol{M})$ magnetic charges and is derived by the following potential problem:

$$\begin{aligned} &\nabla^2\Phi_{in} = \nabla\cdot\boldsymbol{M}, \quad \text{inside } V \\ &\nabla^2\Phi_{out} = 0, \qquad \text{outside } V \end{aligned} \tag{14}$$

and the conditions

$$\begin{aligned} &\Phi_{in} = \Phi_{out} \\ &-\frac{\partial\Phi_{in}}{\partial n} = -\frac{\partial\Phi_{out}}{\partial n} + \boldsymbol{n}\cdot\boldsymbol{M}, \end{aligned} \tag{15}$$

on the boundary ∂V of the ferromagnetic specimen.

Ferromagnetic thin film under mechanical stress

The above formulated magnetomechanical problem is very complicated and thus it is difficult to be solved even under major assumptions. Our aim is to simplify the problem without loosing the underlying physics. Recently a series of experiments were performed in order to show the effect of stress on the hysteresis of ferromagnetic thin films [20-21]. Similar experiments for Ni thin films were also performed by the authors of references [22-24]. SW like models have been used by these authors to explain experimental observations [25]. We assume that:

(i) The width of the thin film $d = 2\alpha$ is in the x direction, and the film is infinitely long in the other two directions y and z.

(ii) The magnetization vector is confined on the Oyz plane and it is only dependent on the distance x from the thin film center, $\boldsymbol{M}: \left(0, M_S\sin(\theta), M_S\cos(\theta)\right)$, $\theta = \theta(x)$.

(iii) The body forces are neglected $(f_i = 0)$.

(iv) The external applied field is along the z axis which is also an easy axis of the crystal $\left(\boldsymbol{H}^\circ: \left(0, 0, H^\circ\right)\right)$.

(v) Infinitesimal deformations are confined to be uniform $\left(e_{ij} = \frac{1}{2}\left(u_{i,j} + u_{j,i}\right),\right.$ $\left. u_i = A_{ij}\,x_j, \quad A_{ij} = A_{ji} = \text{const.}\right)$.

(vi) The crystal is cubic.

(vii) The applied tensile $(T_x > 0)$ or compressive $(T_x < 0)$ stresses are along the x direction.

(viii) Exchange-strictive phenomena are negligible since this is also dictated by available experimental results [20].

(ix) The surface magnetocrystalline anisotropy is considered negligible.

(x) The elastic constants do not change with the magnetization.

The geometry of the problem, after the above assumptions is shown in Fig. 1.

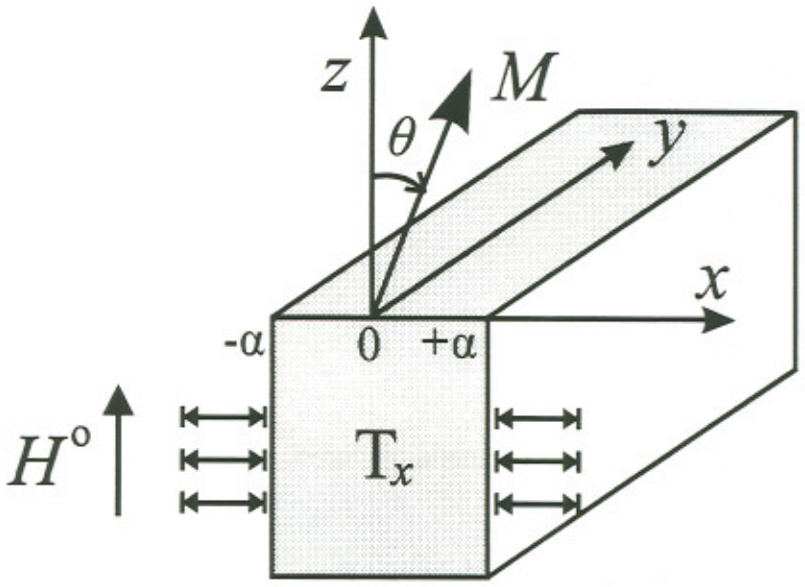

Figure 1: Problem Geometry.

The selection of the magnetization reversal plane (parallel to the boundary surfaces of the thin film) has the advantage of minimizing the magnetostatic free energy and thus the potential problem (14-15) is automatically satisfied. Thus it can be neglected in the further solution of the problem. All the calculations are limited to the case where the mechanical stress is applied perpendicular to the direction of the external field $(\boldsymbol{T} \perp \boldsymbol{H}^{\circ})$. The problem of a mechanical stress applied parallel to the direction of the external field $(\boldsymbol{T} // \boldsymbol{H}^{\circ})$ is mathematically more elaborate due to the presence of magnetic charges on the boundary surface and thus the unavoidable solution of the potential problem (14-15).

Since the crystal is cubic the local part of the free energy can be decomposed into the following parts:

$$F_{loc} = F_{ex} + F_K + F_{el} + F_{mel} \tag{16}$$

where

$$\begin{aligned}
F_{ex} &= \frac{C}{2}\left[(\nabla a_x)^2 + (\nabla a_y)^2 + (\nabla a_z)^2\right] \\
F_K &= K\left(a_x^2 a_y^2 + a_y^2 a_z^2 + a_z^2 a_x^2\right) \\
F_{el} &= \frac{c_{11}}{2}\left(e_{xx}^2 + e_{yy}^2 + e_{zz}^2\right) + \frac{c_{44}}{2}\left(e_{xy}^2 + e_{yz}^2 + e_{zx}^2\right) + c_{12}\left(e_{xx}e_{yy} + e_{yy}e_{zz} + e_{zz}e_{xx}\right) \\
F_{mel} &= B_1\left(a_x^2 e_{xx} + a_y^2 e_{yy} + a_z^2 e_{zz}\right) + 2B_2\left(a_x a_y e_{xy} + a_y a_z e_{yz} + a_z a_x e_{zx}\right).
\end{aligned} \tag{17}$$

3.EFFECT OF STRESS ON MAGNETIZATION.

If the stress tensor t_{ij} is computed from equations (11) and (16-17), it is not difficult to show that the mechanical equilibrium equations (10.1) are automatically satisfied. In this case the mechanical equilibrium problem reduces to the satisfaction of the boundary conditions (10.2). *These boundary conditions give to the model its validity for describing magnetization reversal mechanisms under stress.*

Since $M_n \equiv \boldsymbol{n} \cdot \boldsymbol{M} = 0$, on the boundary surfaces $x = \pm\alpha$ we have:

$$\begin{aligned} t_{xx} n_x &= T_x \\ t_{yx} n_x &= 0 \\ t_{zx} n_x &= 0, \end{aligned} \tag{18}$$

where according to (11) and (17)

$$\begin{aligned} t_{xx} &= c_{11} e_{xx} + c_{12}\left(e_{yy} + e_{zz}\right) + B_1 a_x + \left[2B_1 a_x e_{xx} + 2B_2\left(a_y e_{xy} + a_z e_{zx}\right) + K\left(a_x + a_y\right)\right] a_x \\ t_{yx} &= c_{44} e_{xy} + 2B_2\, a_z a_x + \left[2B_1\, a_y e_{yy} + 2B_2\left(a_x e_{xy} + a_z e_{yz}\right) + K\left(a_x + a_z\right)\right] a_x \\ t_{zx} &= c_{44} e_{zz} + 2B_2\, a_z a_x + \left[2B_1\, a_z e_{zz} + 2B_2\left(a_y e_{yz} + a_x e_{zx}\right) + K\left(a_x + a_y\right)\right] a_x . \end{aligned} \tag{19}$$

Due to the simplifying assumptions, substitution of (19) into (18) leads to

$$\begin{aligned} c_{11} e_{xx} + c_{12}\left(e_{yy} + e_{zz}\right) &= T_x \\ e_{xy} = e_{zx} &= 0. \end{aligned} \tag{20}$$

The magnetic equilibrium problem, after the assumption (ii), reduces to the following set of equations:

$$H_z^{\text{eff}} \sin\theta - H_y^{\text{eff}} \cos\theta = 0 \tag{21.1}$$

$$H_x^{\text{eff}} \cos\theta = 0 \tag{21.2}$$

$$H_x^{\text{eff}} \sin\theta = 0, \tag{21.3}$$

where

$$H_x^{\text{eff}} = -\frac{2B_2}{\mu_o M_S}\left(\sin\theta\, e_{xy} + \cos\theta\, e_{zx}\right) \tag{22.1}$$

$$\begin{aligned} H_y^{\text{eff}} = &-\frac{2K}{\mu_o M_S}\cos^2\theta \sin\theta - \frac{2B_1}{\mu_o M_S} e_{yy} \sin\theta - \\ &-\frac{2B_2}{\mu_o M_S} e_{yz} \cos\theta + \frac{C}{\mu_o M_S}\left[\cos\theta \frac{d^2\theta}{dx^2} - \sin\theta\left(\frac{d\theta}{dx}\right)^2\right] \end{aligned} \tag{22.2}$$

$$H_z^{eff} = H^\circ - \frac{2K}{\mu_o M_S}\sin^2\theta\cos\theta - \frac{2B_1}{\mu_o M_S}e_{zz}\cos\theta - \\ - \frac{2B_2}{\mu_o M_S}e_{yz}\sin\theta - \frac{C}{\mu_o M_S}\left[\sin\theta\frac{d^2\theta}{dx^2} + \cos\theta\left(\frac{d\theta}{dx}\right)^2\right]. \tag{22.3}$$

The equations (22.1) and (21.2-3) lead to

$$H_x^{eff} = 0, \tag{21}$$

which due to (20.2) is automatically satisfied, while substitution of (22.2-3) into (21.1) leads to the differential equation,

$$C\frac{d^2\theta}{dx^2} - 2K\frac{\sin 4\theta}{4} + B_1\left(e_{zz} - e_{yy}\right)\frac{\sin 2\theta}{2} - 2B_2 e_{yz}\cos 2\theta - \mu_o M_S H^\circ \sin\theta = 0. \tag{24}$$

The boundary conditions (12.2) read:

$$\left.\frac{d\theta}{dx}\right|_{x=\pm\alpha} = 0. \tag{25}$$

Thus the problem reduces to the solution of the BVP (24-25) and (20.1). We introduce the following dimensionless parameters:

$$\bar{x} = x/\alpha, \quad h_k = \frac{2K}{\mu_o M_S^2}, \quad h_1 = \frac{B_1}{\mu_o M_S^2}, \quad h_2 = \frac{B_2}{\mu_o M_S^2}, \quad h = \frac{H^\circ}{M_S}, \\ S = \frac{\alpha}{R_o}, \quad \sigma = \frac{T_x}{\mu_o M_S^2}, \quad h_3 = \frac{c_{11}}{\mu_o M_S^2}, \quad h_4 = \frac{c_{12}}{\mu_o M_S^2}, \quad h_5 = \frac{c_{44}}{\mu_o M_S^2} \tag{26}$$

where

$$R_o \equiv \sqrt{\frac{C}{\mu_o M_S^2}} = \sqrt{\frac{2A}{\mu_o M_S^2}} \tag{27}$$

is the exchange length.

Then the BVP (24-25) and (20.1) takes the following form

$$\frac{d^2\theta}{d\bar{x}^2} - h_k S^{-2}\frac{\sin 4\theta}{4} + h_1 S^{-2}\left(e_{zz} - e_{yy}\right)\sin 2\theta - h_2 S^{-2} e_{yz}\cos 2\theta - hS^{-2}\sin\theta = 0, \\ \left.\frac{d\theta}{d\bar{x}}\right|_{\bar{x}=\pm S} = 0, \\ h_3\, e_{xx} + h_4\left(e_{yy} + e_{zz}\right) = \sigma. \tag{28}$$

Like all one dimensional micromagnetic problems the Brown's equation (28.1) can be integrated at least once [26],

$$\frac{1}{2}\left(\frac{d\theta}{d\bar{x}}\right)^2+\frac{h_k}{S^2}\frac{\cos 4\theta}{8}+\frac{h_1}{S^2}\left(e_{yy}-e_{zz}\right)\frac{\cos 2\theta}{2}-\frac{h_2}{S^2}e_{yz}\frac{\sin 2\theta}{2}+\frac{h}{S^2}\cos\theta=\frac{A_1}{8}, \tag{29}$$

where A_1 is an integration constant. Equation (29) can equivalently be written in the following form

$$\int_{\theta_0}^{\theta}\frac{d\theta}{\sqrt{A_1-h_k\cos 4\theta-4h_1\left(e_{yy}-e_{zz}\right)\cos 2\theta+4h_2e_{yz}\sin 2\theta-8h\cos\theta}}=\frac{\bar{x}}{2S}, \tag{30}$$

which is an elliptic type integral that, under appropriate conditions, can be calculated even analytically. It is obvious that the initial saturation state $\theta_{in}(x)=0$ ***is not*** a solution of the BVP (24-25). It is a solution if we assume that $e_{yz}\cong 0$. Thus in the following we will concentrate our attention on solutions with strain tensor,

$$e_{ij}=\begin{pmatrix} e & 0 & 0\\ 0 & e & 0\\ 0 & 0 & 0\end{pmatrix}, \tag{31}$$

where we have additionally assumed that $e_{zz}\cong 0$ and $e_{xx}\cong e_{yy}=e$. This is a legitimate assumption since the applied mechanical stresses are along the x direction. In general the strain tensor e_{ij} has contributions from intrinsic strains due to spontaneous magnetostriction e_{ij}^{intr}, as well as external strains from mechanical deformations e_{ij}^{mech}. In the following we assume that the intrinsic mangetostrictive strains are negligible compared to the forced mechanical strains due to applied stresses. This is justified because magnetostrictive in origin strains are of the order of $e_{ij}^{intr}=\mathrm{O}\left(10^{-6}\right)$ while the mechanical ones are $e_{ij}^{mech}\geq 10^{-4}$. Then the boundary condition (28.3) reduces to the following linear relation between the applied stress and the strain

$$\sigma=\left(h_3+h_4\right)e. \tag{32}$$

3.1 COHERENT REVERSAL

We first seek for solutions of uniform magnetization reversal. These modes of reversal were first proposed by Stoner and Wolfarth [27] for single domain particles.

Equation (28.1) reduces to

$$h = -\frac{h_k \sin 4\theta + 4h_1 e \sin 2\theta}{4\sin\theta}. \tag{33}$$

The hysteresis curve is defined as the mean magnetization along the applied field direction

$$M_H \equiv \frac{1}{V}\iiint_V \boldsymbol{M}\cdot\vec{\boldsymbol{e}}_H\, dV. \tag{34}$$

Thus for the problem under discussion

$$m = \cos\theta, \quad m \equiv M_H / M_S. \tag{35}$$

Hysteresis curves based on the parametric set of equations (33) and (35) are plotted in Fig. (2) for zero applied stresses:

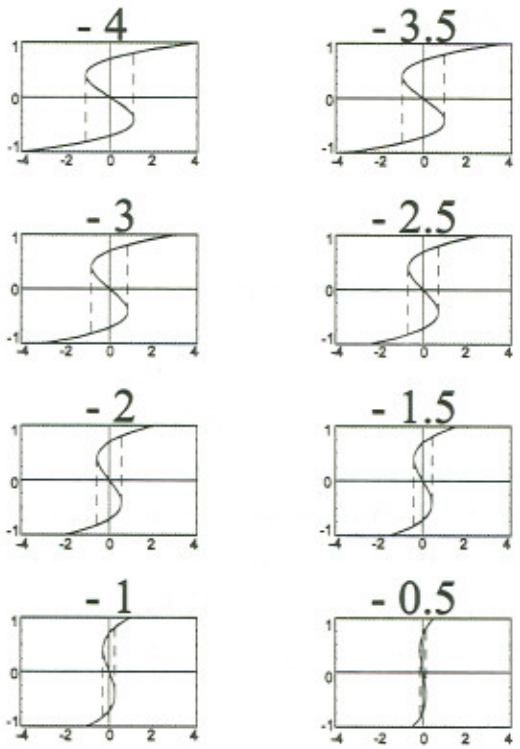

Figure 2: Hysteresis loops for coherent magnetization reversal for $\sigma = 0$, $h_1 = 500$, and various reduced anisotropy constants, $h_k \in [-4, 0)$.

The horizontal axis in Fig. 2 is the axis of the reduced applied field h, and the vertical one is the axis of the reduced magnetization m. The dashed lines denote the irreversible jump of the magnetization from the one stable saturation state to the other, since the hysteresis loop corresponds to positive susceptibilities $(\partial m/\partial h > 0)$.

It is generally acceptable that applied stresses produce easy axis (EA) of magnetization. Thus in many calculations the magnetostrictive effects are considered as another form of magnetic anisotropy. If on a previous demagnetized ferromagnetic specimen we apply mechanical stresses an EA of magnetization emerges as shown in Fig. 3 for materials with positive and negative magnetostriction λ_s, under tensile $(\sigma > 0)$, or compressive stresses $(\sigma < 0)$.

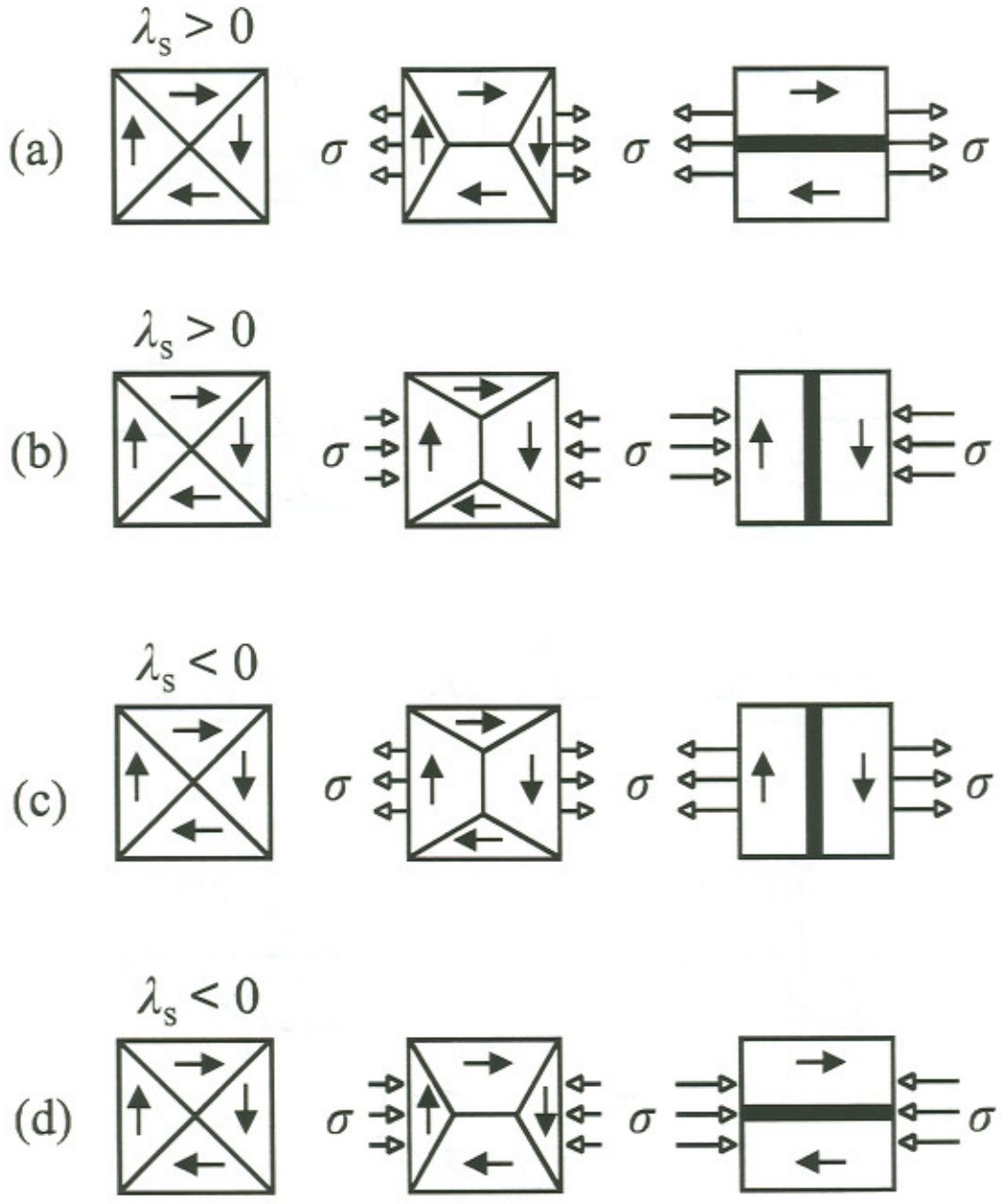

Figure 3: Easy Axis formation due to stress (The easy axis is indicated with the thick line)(schematic).

As it is shown in Fig. 3, for materials with positive magnetostriction a tensile stress produces an EA along the direction of the applied stress (Fig. 3a), while the same applied stress in a material with negative magnetostriction produces an EA perpendicular to the direction of the applied stress (Fig. 3c). These are experimental

observations that must be justified by the theory. In related experiments [20-24] it is observed, that for materials with negative magnetostriction (like Ni) an applied tensile or compressive stress increases or decreases, respectively, the coercivity, if the external field is applied perpendicular to the direction of the stress. All possible effects of stresses on the coercivity are shown in Fig. 4 for materials with negative magnetostriction.

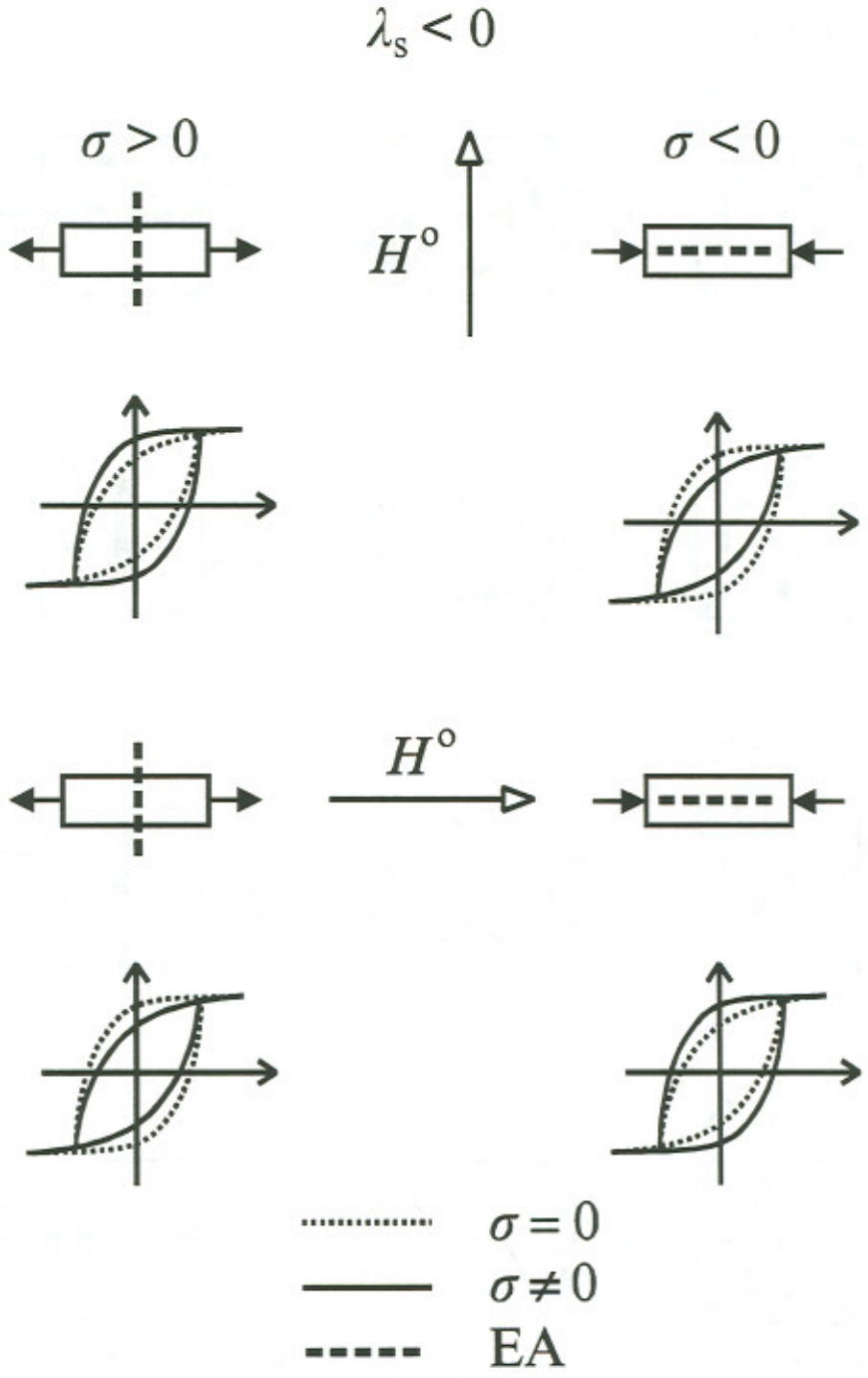

Figure 4: Effect of stress on coercivity for materials with negative magnetostriction, with the external field applied parallel or vertical to the stress direction (schematic).

The situation is exactly the opposite for materials with positive magnetostriction.

The condition $e \neq 0$ corresponds to non-vanishing applied stresses and the second term on the numerator of the right hand-side of equation (33) changes sign for tensile or compressive stress, and this affects the whole hysteresis curve, as it is evident in Fig. 5, for just one set of parameters.

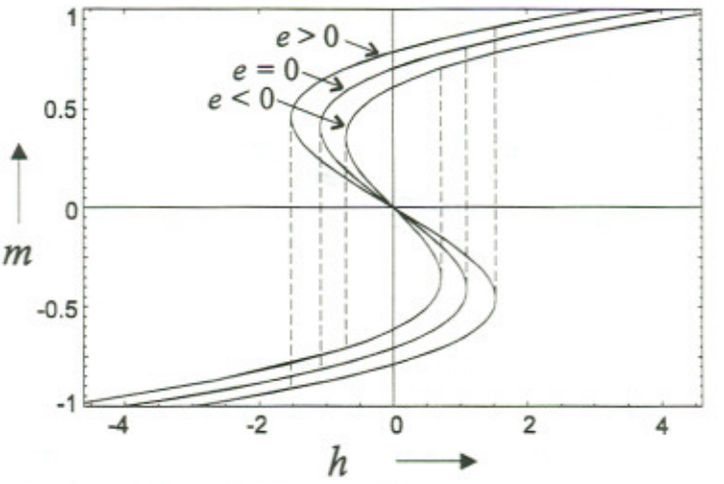

Figure 5: Hysteresis loops for $\sigma \neq 0$ (tensile $e > 0$ and compressive $e < 0$) for $h_k = -4$, $h_1 = 5\times10^3$ and $|e| = 10^{-4}$.

It is obvious from Fig. 5 that stress alters the magnetic characteristics of the thin film. This corresponds to material with negative magnetostriction, like Ni. In this case $h_1 > 0$, for materials with positive magnetostriction $(h_1 < 0)$ the situation in Fig. 5 is exactly the opposite. It is obvious from equation (33) that increment of h_1 by an order of magnitude and decrement of e by an order of magnitude do not alter the stress dependence on coercivity since both of them appear in (33) as a multiplication product. A family of hysteresis curves for tensile and compressive stress for $|e| = 10^{-4}$ are plotted in Figs. 6 and 7, respectively (dashed lines). In the same figures the related hysteresis curves for zero stress (solid lines) are also presented for comparison.

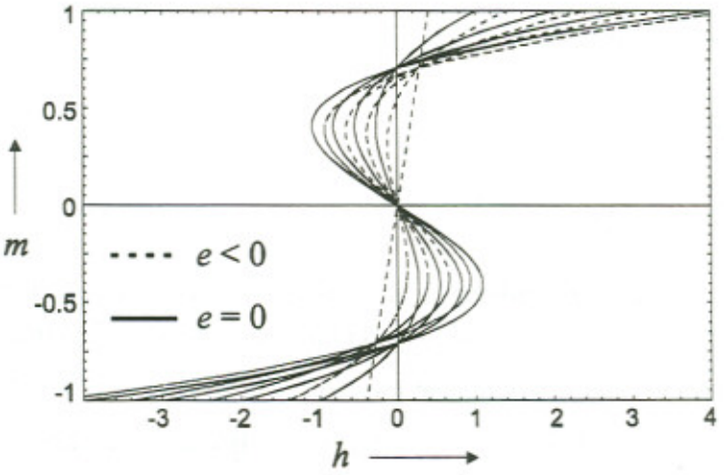

Figure 6: Hysteresis loops for $e = -10^{-4}$, $h_k \in [-4, 0]$ and $h_1 = 2\times10^3$. The related hysteresis loops for $e = 0$ are also shown for comparison (solid lines).

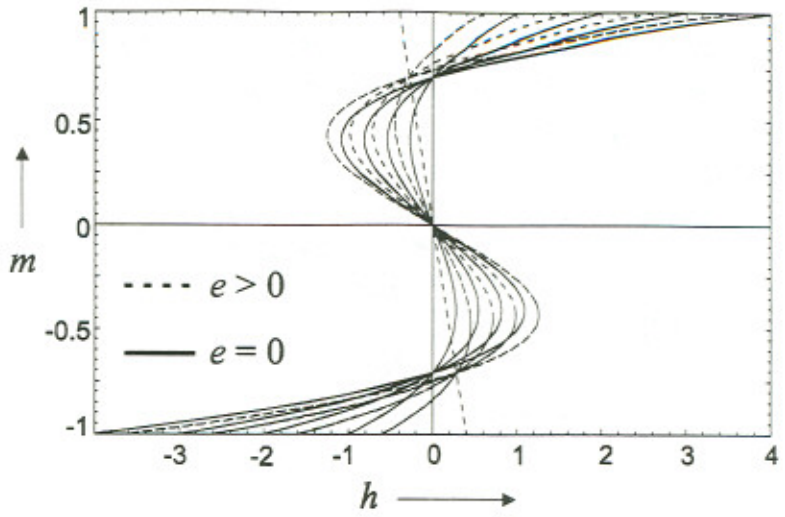

Figure 7: Same as Fig. 6 with $e = 10^{-4}$

In Figs. 6 and 7 the regions with negative slope should also be considered undesirable from physical reasoning $(\partial m/\partial h > 0)$. The irreversible jumps at these points are not shown to avoid difficulties in reading the figures. The straight dashed lines in Figs. 6 and 7 correspond to zero magnetocrystalline anisotropy $(h_k = 0)$. Thus, under the simplifying assumptions of our model, materials with negligible magnetocrystalline anisotropy and negative magnetostriction, that reverses their magnetization uniformly, have non-hysteretic behavior under compressive stress and rectangular hysteresis loops for tensile stress applied perpendicular to the direction of the external field.

3.1.1 THE $h_c = h_c(\sigma)$ LAW

It is not difficult to show that equation (33) can be written as

$$h = -\cos\theta\left(2h_1 e + h_k \cos 2\theta\right), \tag{36}$$

or due to (35) as

$$h = h(m) = -m\left(2h_1 e + h_k\left(2m^2 - 1\right)\right). \tag{37}$$

Equation (37) can also be inverted, in order to obtain the constitutive relation $m = m(h)$, but it is not really needed in order to obtain the law that relates the reduced coercive force $\left(h_c \equiv H_c / M_s\right)$ and the reduced stress σ. Under the above mentioned assumptions the reduced free energy $\left(g \equiv G/\left(\mu_o M_s^2\right)\right)$ can be written as

$$g = g(\theta) = \mathrm{f}_{\mathrm{loc}}(\theta) - h\cos\theta, \tag{38}$$

with

$$f_{loc}(\theta) \equiv \frac{F_{loc}}{\mu_0 M_S^2} = h_k \frac{\sin^2 2\theta}{8} + h_1 e \sin^2\theta + (h_3 + h_4)e^2, \tag{39}$$

or by invoking (eq. (32)), as:

$$f_{loc}(\theta) = h_k \frac{\sin^2 2\theta}{8} + \frac{h_1}{h_3 + h_4}\sigma \sin^2\theta + \frac{\sigma^2}{h_3 + h_4} \tag{40}$$

Then we can relate the slope of the magnetization curve $\partial m/\partial h$ with the second derivative of the free energy with respect to θ as follows:

$$\frac{\partial h}{\partial m(\theta)} = [m'(\theta)]^2 g''(\theta), \tag{41}$$

where $(\,)' \equiv d/d\theta$. The sign of $g''(\theta)$ is therefore the sign of the slope of the hysteresis curve. Thus sections of the curve with positive slope represent stable states; and sections with negative slope, unstable states. At the point of infinite slope $(\partial m/\partial h = \infty)$ the magnetization reverses irreversibly from the one equilibrium state to the other. This point corresponds to the coercive force h_C and is expressed by

$$\frac{\partial h}{\partial m} = 0. \tag{42}$$

But due to (37) equation (42) leads to:

$$m_C = \pm\sqrt{\frac{h_k - 2h_1 e}{6h_k}}. \tag{43}$$

Substitution of (43) into (37) results in the coercive field

$$h_C(\sigma) = \frac{1}{3}\sqrt{\frac{2}{3h_k}}\left(h_k - \frac{2h_1}{h_3 + h_4}\sigma\right)^{3/2}. \tag{44}$$

We note that the coercivity does not depend on the thickness of the thin-film S, due to the assumptions made. Generally, coercivity decreases with increasing thin-film thickness. Equation (44) is a rational upper bound for the actual observed coercivity as a function of σ. It should agree well with experimental results for thin films with thickness $d = 2\alpha \le 500\,nm$. For materials with negative magnetostriction $(\lambda_{100} < 0 \Leftrightarrow h_1 > 0)$ and negative magnetocrystalline anisotropy $(h_k < 0)$ the law (44) predicts an increase of coercivity for tensile stresses $(\sigma > 0)$ and a decrease for compressive stresses $(\sigma < 0)$. The law (44) is valid only when the directions of applied

stress and external field are perpendicular to one another $(\sigma \perp h)$. This is what actually was observed in the experiments by Han, Zhu, Judy and Sivertsen [20-21] and Callegaro and Puppin [22].

We can compare the results obtained by (44) for Ni thin film of thickness $d = 2\alpha = 20\ nm$, since for this particular case there are available experimental results [22]. The material constants for Ni are given on Table 1

Constant	SI
λ_{100}	-50×10^{-6}
λ_{111}	-20×10^{-6}
c_{11}	$2.48\times10^{11}\left(N/m^2\right)$
c_{12}	$1.53\times10^{11}\left(N/m^2\right)$
c_{44}	$1.16\times10^{11}\left(N/m^2\right)$
M_S	$39.79\left(kA/m\right)$
K	$-4.26\times10^{3}\left(J/m^3\right)$
C	$6.8\times10^{-12}\left(J/m\right)$

Table 1: Material constants for Ni [28].

For deformable ferromagnetic specimens we have

$$M_S = \rho \mathsf{M}_S \left(1 - u_{i,i}\right). \tag{45}$$

In the case under discussion

$$u_{i,i} \cong 2e \tag{46}$$

and $e \cong O\left(10^{-4}\right)$, therefore we accept that,

$$M_S \cong \rho \mathsf{M}_S \cong const. \tag{47}$$

We note that for uniformly magnetized specimens the magnetoelastic constants are given by [6]:

$$\begin{aligned} B_1 &= -\frac{3}{2}\lambda_{100}\left(c_{11} - c_{12}\right) \\ B_2 &= -\frac{3}{2}\lambda_{111}\, c_{44}, \end{aligned} \tag{48}$$

and due to (26) we have

$$h_1 = -\frac{3}{2}\lambda_{100}\left(h_3 - h_4\right)$$
$$h_2 = -\frac{3}{2}\lambda_{111}\, h_5 . \tag{49}$$

For Ni the dimensionless quantities have values shown in Table 2, for a thin film of thickness $d = 2\alpha = 20\ nm$.

S	h_k	h_1	h_2	h_3	h_4
0.17	-4.28	3581	1749	124658396	76906188

Table 2: Dimensionless parameters for Ni.

The coercivity values based on (44) are compared with experimental values [22] and the results are cited in Table 3.

$T_x\ (MPa)$	$\sigma\left(=T_x/\mu_0 M_S^2\right)$	$H_C^{exp}\ (Oe)$	$h_C^{exp}\left(=H_C^{exp}/M_S\right)$	h_C (eq.(44))
-125	-62832	131.1	0.262	0.3860
-100	-50265	132.7	0.265	0.519
-62	-31164	134.3	0.269	0.744
0	0	140	0.280	1.166
35	17593	144.1	0.288	1.430
70	35186	147.1	0.294	1.712
85	42726	148.6	0.297	1.837
100	50265	156.2	0.312	1.966

Table 3: Coercivity according to (44) and [22] for Ni thin film of thickness $d = 2\alpha = 20\ nm$.

It is obvious that the theoretical coercive force is always an upper bound of the experimentally measured one. For large compressive stresses the gap between theoretical predictions and experimental results is minimized. The disagreement between theory and experiment is evident. This is mainly due to the fact that the strains are not in general uniform as it was assumed in the above calculations. In addition the material is finite and thus magnetostatic effects alter the picture of uniform magnetization and the material is not defect-free in the sense that there are always imperfections that serve as nucleation centers which decrease coercivity. Therefore it is expected that for thinner films than those used in [20-22] the law (44) is applicable. One can use equation (44) as a fitting law to experimental results for thin films in order to calculate the magnetostriction constant λ_{100}, provided that the elastic and anisotropy constants are known. In that case due to (49.1) equation (44) gives:

$$h_C(\sigma) = \frac{1}{3}\sqrt{\frac{2}{3h_k}}\left(h_k + 3\lambda_{100}\frac{h_3 - h_4}{h_3 + h_4}\sigma\right)^{3/2}. \tag{50}$$

One can also assume that the applied stress alters the character of the magnetocrystalline anisotropy and thus equation (44) can be used as a fitting law to the experimental results, in order to determine the mangetocrystalline anisotropy, provided the elastic and magnetostrictive constants are given. We will not examine these cases further.

3.1.2 THE $m_R = m_R(\sigma)$ LAW

Due to eq. (37) we can compute the remanence as a function of stress. The remanence corresponds to $h = 0$ and thus using (37) we obtain, in dimensionless form $\left(m_R \equiv M_R / M_S\right)$,

$$m_R = \pm \sqrt{\frac{1}{2} - \frac{h_1 \sigma}{h_k \left(h_3 + h_4\right)}}. \tag{51}$$

For materials with negative magnetostriction $\left(h_1 > 0\right)$ and negative magnetocrystalline anisotropy $\left(h_k < 0\right)$ (like Ni), equation (51) predicts that the remanence increases for tensile stress and decreases for compressive. This shows the same qualitative behavior as experimental observations [20-22]. We note that equation (51) was obtained for mechanical stresses that were applied perpendicular to the direction of the external field $\left(\sigma \perp h\right)$. Typical results for Ni are shown in Fig. 8.

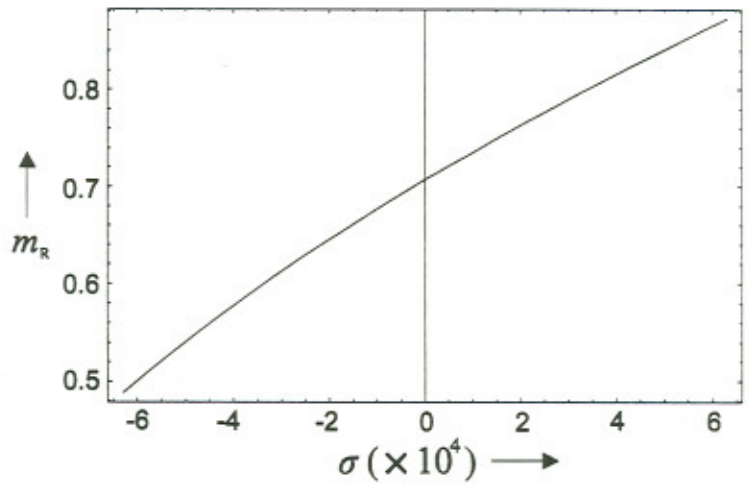

Figure 8: Remanence m_R as a function of stress σ. The material constants correspond to Ni.

The energy is plotted in Fig. 9 as a function of θ with the applied field as a parameter.

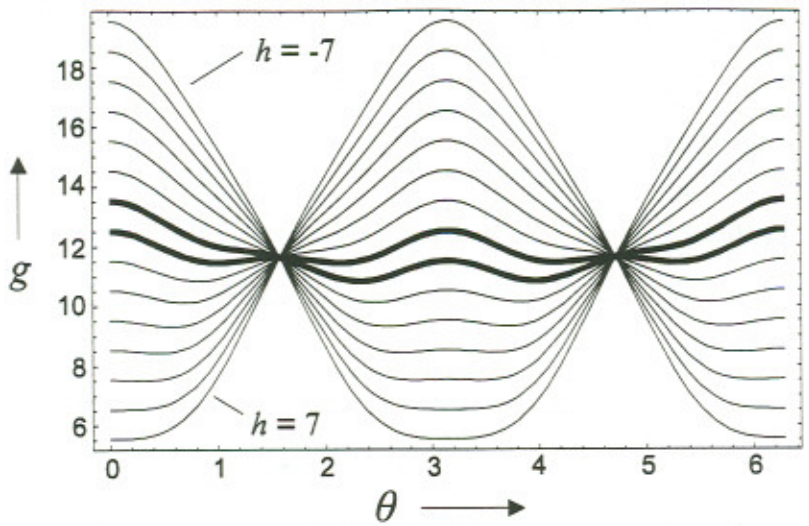

Figure 9: Energy as a function of θ for various applied fields $h \in [-7, 7]$ with step 1 and for an applied compressive stress $\sigma = -50265$. The material constants correspond to Ni.

It is obvious from Fig. 9 that for large positive fields the initial saturation state along the direction of the applied field $(\theta = 0)$ is the stable equilibrium state, while for large negative fields the saturation along the reversed field $(\theta = \pi)$ is a stable equilibrium state. When the field is reduced from large positive values, metastable states emerge. For negative fields those metastable states are responsible for the irreversible jump at $h = h_c$. The bold curves correspond to fields before $(h = 0)$ and after $(h = -1)$ the irreversible jump at $h_c = -0.519$. In Fig. 10 the situation is the same as that of Fig. 9 with the difference that we now plotted the energy as a function of the magnetization m.

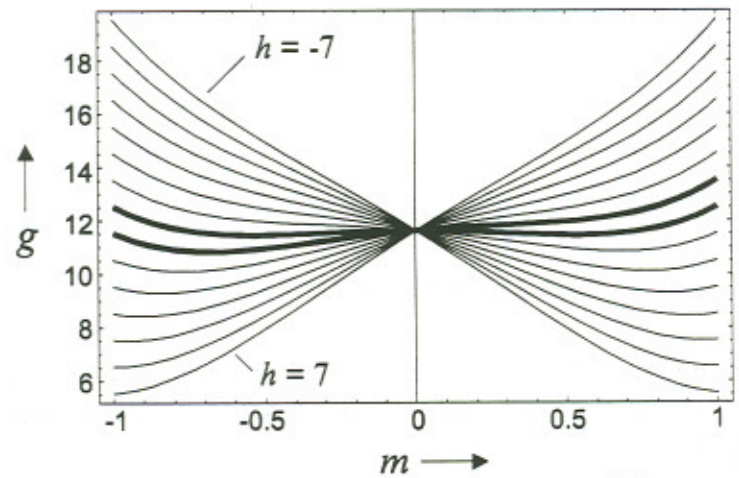

Figure 10: Same as Fig. 9 with $g = g(m)$.

The energy profiles for equilibrium solutions (equation (38) with h given by (36)) are plotted in Fig. 11 as a function of the angle θ for various applied stresses.

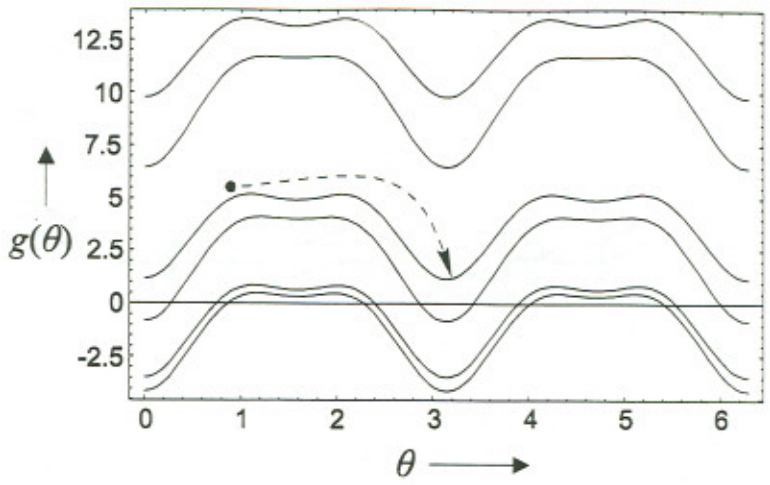

Figure 11: Energy equilibrium profiles as a function of θ for various stresses.

It is obvious that the two saturation states of uniform magnetization $\theta = 0$ and $\theta = \pi$ along the direction of the applied field are equilibrium states. The irreversible transition at the point of infinite permeability $(h = h_c)$ to the other equilibrium state $\theta = \pi$ is also marked in Fig. 11. The same situation is shown in Fig. 12 where instead of the free energy we plot its second derivative.

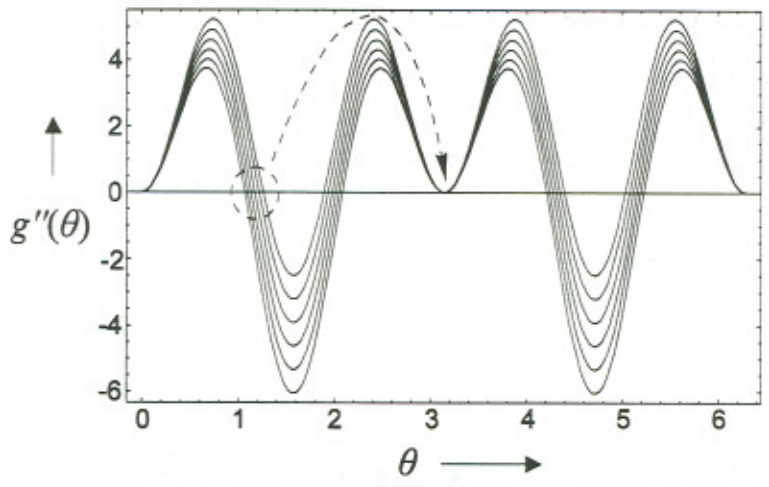

Figure 12: Same as figure 11 with $g''(\theta)$ instead of $g(\theta)$.

Irreversible transition regions $(g''(\theta) = 0)$ at $h = h_c$ are also marked as in Fig. 11. The hysteresis curve for the material parameters that correspond to Ni are plotted in Fig. 13 for various stresses.

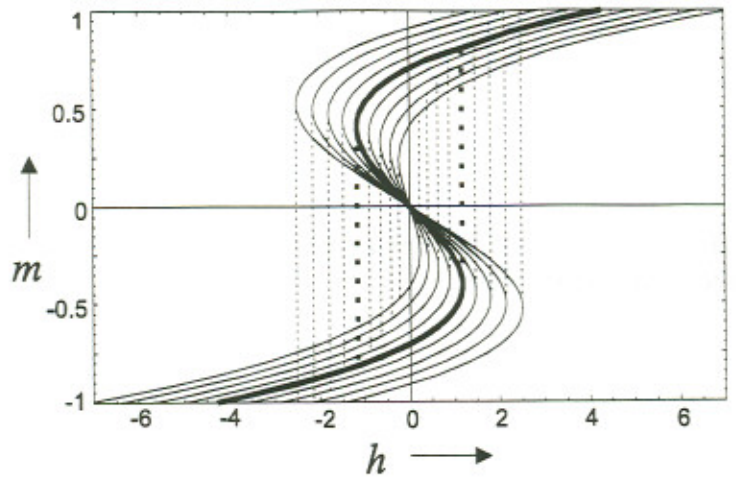

Figure 13: Hysteresis curves for varying stresses $\sigma \in \left[-8, 8\right] \times 10^4$ with step 2×10^4. The material parameters correspond to Ni. The bold curve correspond to zero applied stresses $(\sigma = 0)$.

We summarize in Table 4 the upper and lower bounds for stress and coercivity of Fig. 13.

$\sigma\ (\times 10^4)$	h_C	$T_x\ (MPa)$	$H_C\ (kA/m)$	$H_C\ (Oe)$
-8	0.227	-159	9.03	113.5
8	2.501	159	99.51	1250.5

Table 4: Coercivities and stresses for Fig. 13. The material constants correspond to Ni.

It is deduced from Fig. 13 that the application of a tensile stress on a material with negative magnetostriction and negative magnetocrystalline anisotropy, apart from increasing the coercivity, it also increases the remanence and the deviation from the initial saturation state appears at lower fields. These are experimentally observed facts too [21]. The opposite happens with the application of a compressive stress.

3.2 NON-UNIFORM REVERSAL

Linearized Problem (Nucleation field calculation)

Some first conclusions about the mode of departure from the initial saturation state along the direction of the applied field can be derived by the linearized form of equation (28.1-2) which is the following:

$$\frac{d^2\theta}{d\bar{x}^2} - k^2\theta(\bar{x}) = 0, \tag{52}$$

with

$$k^2 \equiv \left(h + h_k - h_1 e\right) S^{-2}. \tag{53}$$

The general solution of (52) is

$$\theta(\bar{x}) = C_1 e^{k\bar{x}} + C_2 e^{-k\bar{x}}. \tag{54}$$

(The exponential in (54) should not be confused with the strains). The constants are determined from the boundary conditions (28.2):

$$\begin{aligned} k C_1 e^{kS} - k C_2 e^{-kS} &= 0 \\ k C_1 e^{-kS} - k C_2 e^{kS} &= 0 \end{aligned} \tag{55}$$

Non vanishing solution to the set of equations (55) exists when

$$k^2 \sinh(kS) = 0. \tag{56}$$

Equation (56) determines the nucleation field. Thus from (56)

$$k = 0 \tag{57}$$

and due to (53) we obtain the following linear relation between the nucleation field and the applied stress

$$h_N = -h_k + h_1 e. \tag{58}$$

The derived law $h_N = h_N(\sigma)$ has already been used for the interpretation of stress dependence on coercivity for iron whisker by Self et al. [29]. We note that the typical theoretical value of the nucleation field $-h_k$ is modified by the second term in (58) due to applied stresses and it does not depend on size. This is mainly due to the oversimplification of the problem. In Fig. 14 we plot the reduced coercivity and the reduced nucleation field, as a function of the applied stress and the results are compared with experimental observations [22].

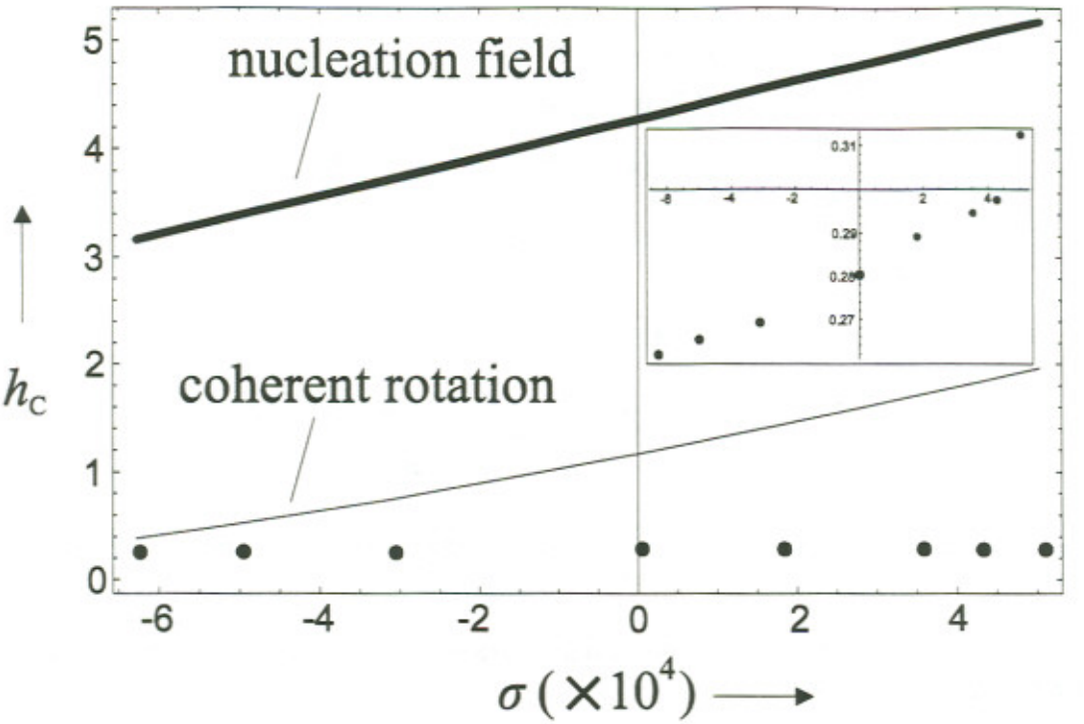

Figure 14: Reduced coercivity as a function of stress. The material constants correspond to Ni. The dots correspond to experimental data of Callegaro et al [22].

Figure 14 is misleading, in the sense that shows that the experimental data are independent of stress. This is not actually true as the enclosed framed figure shows. What is remarkable is that the theoretically predicted coercivity is always an upper bound of the experimental results. One can fit the available experimental values of coercivity (Table 3) to equations (50) and (58) in order to calculate the anisotropy and magnetostriction constants for Ni, provided that the elastic constants are known. The results are summarized in Table 5.

	Eq. (50)	Eq. (58)
$K\,(J/m^3)$	-1034.90	-281.80
$\lambda_{100}\,(\times 10^{-6})$	-1.35	-1.09

Table 5: Material constants for Ni.

The values calculated by equation (50) are closer to the tabulated values (Table 1), compared to the values obtained from equation (58). The higher discrepancy obtained from the fitting by equation (58) is due to the fact that this equation computes the nucleation field and not the coercivity. The nucleation field is always an upper bound of the true coercive force that is computed by solving the non-linear problem. However, this is out of the scope of the present work. The fitting of the experimental data to those based on eq. (50) is also shown graphically in Fig. 15.

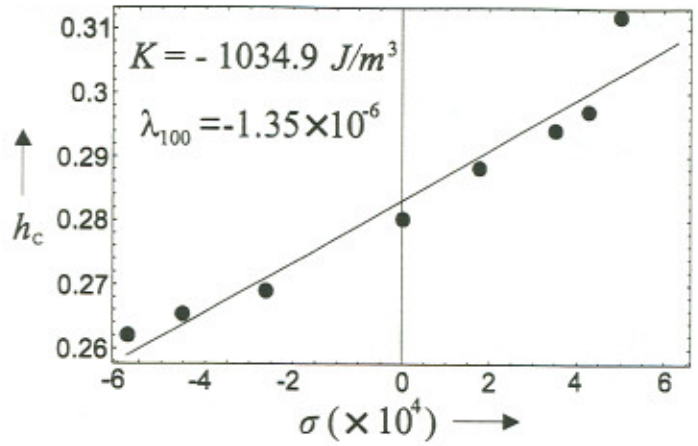

Figure 15: Reduced coercivity as a function of stress (eq. (50)). The dots correspond to experimental data of Callegaro et al [22].

The modes of departure from the initial saturation state along the direction of the applied field correspond, due to (57), to

$$\theta(\bar{x}) = \theta_o = const. \tag{59}$$

Thus, in the present model, the magnetization vector deviates uniformly from the initial saturation state $\theta_{in}(\bar{x}) = 0$, and the thin film, perhaps, behaves like a ferromagnetic particle that remains single domain throughout the magnetization reversal. The non-uniform reversal problem is under investigation and it will be presented in a future communication.

4. CONCLUDING REMARKS

The theory of magnetoelastic interactions, originally proposed by Brown [2] was utilized in order to describe the magnetization reversal for thin-ferromagnetic films that undergo mechanical loading. Due to its complexity this theory is difficult to be applied to specific problems. For uniform rotation of the magnetization and for applied stresses perpendicular to the direction of the external field, analytical coercivity-stress $h_c(\sigma)$ and remanence-stress $m_R(\sigma)$ relations were derived which explain qualitatively the experimental results. The model predicts that for an applied tensile stress on a material with negative magnetostriction, and with the direction of stress perpendicular to the direction of the external field, the coercivity and remanence increase and the deviation of the magnetization from the initial saturation state along the field direction is performed for lower fields with respect to the stress free state. The opposite is also deduced for compressive stresses. Those predictions show the same qualitative behavior with the experimental observations. The theoretically computed coercivity is always an upper bound of the measured one. Due to the assumption made the $h_c(\sigma)$

law does not include the size dependence on coercivity. We note that the model is subjected to further improvements by assuming non-uniform magnetization reversal mechanisms. The case of non vanishing surface magnetic charges can also be studied, after carefully improving the model, in order to explain the magnetization reversal for thin films with applied stresses parallel to the direction of the applied field.

REFERENCES

[1] A. Aharoni, Introduction to the Theory of Ferromagnetism (Oxford University Press, NY, 1996).
[2] W. F. Brown, Magnetoelastic Interactions (Springer Tracts in Natural Philosophy Vol.9), Edited by C. Truesdell, (Springer Berlin,1966).
[3] A. C. Eringen and G. A. Maugin, Electrodynamics of Continua I-II, (Springer-Verlag, NY, 1990). G. A. Maugin, Continuum Mechanics of Electromagnetic Solids, (North-Holland, Amstredam, 1988).
[4] Tiersten, J. Math. Phys.5 (1964) 1298.
[5] H. F. Tiersten, J. Math. Phys.6 (1965) 779.
[6] Brown, Micromagnetics (John Wiley & Sons,1963).
[7] G. A. Maugin and A. C. Eringen, J. Math. Phys.13 (1972) 143.
[8] G. A. Maugin and A. C. Eringen, J. Math. Phys.13 (1972) 1334.
[9] G. A. Maugin, Relativistic Continuum Physics: Micromagnetism (in Continuum Physics II.), editied by A. C. Eringen, (Academic Press, N.Y.,1975).
[10] A. Misra and B.G. Varshney, J. Mag. Mag. Mat., 89 (1990) 159.
[11] F. C. Moon, Magnetosolid Mechanics (John-Wiley & Sons, NY, 1984) (p. 37).
[12] R. D. James & D. Kinderleher, Cont. Mech. & Therm. 2 (1990) 215.
[13] R. D. James & D. Kinderleher, Phil. Mag. B, 68 (1993) 237.
[14] A. de Simone, Arch. Rat. Mech. Anal., 125 (1993) 99.
[15] P. A. Voltairas, Field Matter Interactions in Ferromagnetic Bodies, (University of Ioannina, Dissertation thesis (in Greek), 1994).
[16] C. V. Massalas and P. A. Voltairas, J. Mag. Mag. Mat., 135 (1994) 271.
[17] R. M. Bozorth, Ferromagnetism, (D. van Nostrand coorp. Inc., NY, 1951) (p. 648).
[18] S. Motogi, Mater. Sci. Forum, 123-125, (1993) 257.
[19] S. Motogi and G. A. Maugin, J. Phys. D: Appl. Phys. 26 (1993) 1459.
[20] De -Hua Han et al., Appl. Phys. Lett. 70 (1997) 664.
[21] De -Hua Han et al., J. Appl. Phys. 81 (1997) 4519.
[22] Callegaro L. et al. Appl. Phys. Lett. 68 (1996) 1279.
[23] J. Nowak et al., J. Appl. Phys. 79 (1996) 3175.
[24] E. Puppin et al, IEEE Trans. Mag. 32 (1996) 281.
[25] Callegaro L et al., IEEE Trans. Mag. 33 (1997) 1007.
[26] W. F. Brown and Shtrikman S., Phys. Rev. 125 (1962) 825.
[27] Stoner E.C. and Wohlfarth E.P., Phil. Trans. Roy. Soc. London, A240, (1948) 599. Reprint in IEEE Trans Magnetics, 27, (1991) 3475.
[28] Landolt-Börnstein, Magnetic properties III (Springer-Berlin, 1962).
[29] Sefl W.B. et al., J. Appl. Phys. 43 (1972) 199.